



Evaluation of Cloud Influences on Aerosol Retrieval and Effects on Radiative Forcing using MODIS and Airborne Measurements During INTEX-B

D. Allen Chu (UMBC/NASA GSFC), Lorraine Remer (NASA GSFC), Philip Russell (NASA ARC), and Edward Browell (NASA LaRC)



Motivation

MODIS aerosol products have been widely used in climate related researches. However, the retrievals do not account properly for elevated aerosols especially over clouds. An example of smoke layers at 5 km over clouds in INTEX-A depicts overestimated aerosol optical depth (AOD) compared to NASA Ames airborne tracking sunphotometer (AATS) measurements. The smoke originated from Alaskan/Canadian fires in summer 2004 appeared to reduce reflectance and thus impair cloud-screening process (left panel in Figure 1). It is clear that MODIS-derived AOD values exceed those observed by AATS over the entire spectrum from visible to near infrared (lower right panels in Figure 1). The chance is rare to obtain the ground truth of AOD over clouds. Field campaign measurements provide the key to studying cloud influences on aerosol retrieval and assessing the effects on radiative forcing.

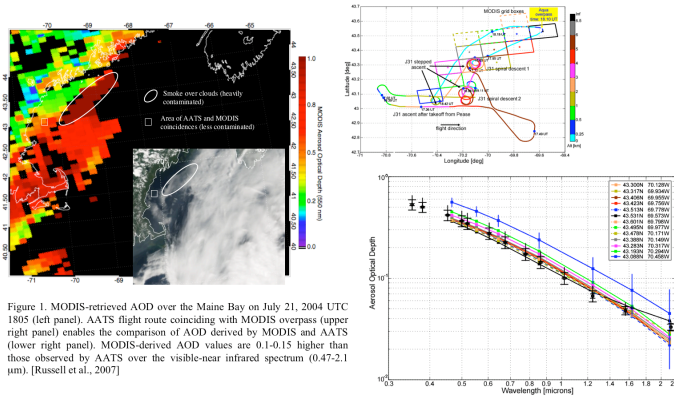


Figure 1. MODIS-retrieved AOD over the Maine Bay on July 21, 2004 UTC 1805 (left panel). AATS flight route coinciding with MODIS overpass (upper right panel) enables the comparison of AOD derived by MODIS and AATS (lower right panel). MODIS-derived AOD values are 0.1-0.15 higher than those observed by AATS over the visible-near infrared spectrum (0.47-2.1 μm). [Russell et al., 2007]

Background

INTEX-B field campaign was conducted in spring 2006, during which the easterly outflow were the strongest to carry dust-laden air mass in long distance and to reach as far as the US and beyond. Under the condition of strong dust outbreaks, nearly the whole Northern Pacific Ocean is covered by dust, mixed with urban/industrial pollution and biomass-burning aerosols as moving out of desert source regions. The year 2006, as found, is as strong as the year 2001 for dust outbreaks. A total of 13 dust outbreaks were recorded in 2006 compared to 15 in 2001. The results shown in Figure 2 illustrates the comparisons of AOD between MODIS and GOCART over the Northern Hemisphere in April 2001. MODIS AOD values are higher than those derived from GOCART especially over the Northeastern Pacific Ocean (INTEX-B domain). A recent comparison showed that MODIS zonal mean AOD values are significantly higher at latitudes $> 40^\circ$ against CMAQ (EPA) and GOCART in both April and May 2001 (Figure 3).

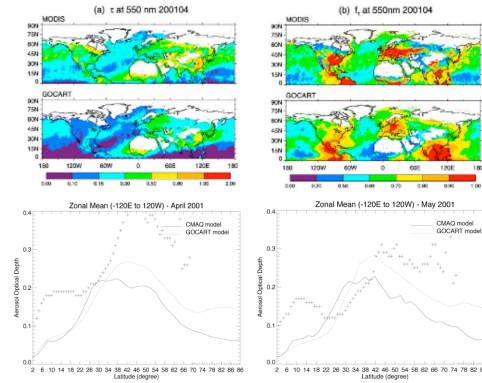


Figure 2. Comparisons of MODIS and GOCART-derived monthly mean AOD (left panels) and fine-mode fraction (right panels) over the Northern Hemisphere in April 2001 [Chin et al., 2004]. Despite the similar pattern of aerosol distribution, MODIS AOD values are higher by at least 0.1 at latitudes $> 40^\circ$ in the Northeastern Pacific where the fine-mode fraction also appears to be larger (either real or due to aerosol model selection issue).

Figure 3. Comparisons of zonal mean AOD from MODIS, GOCART, and CMAQ over the Northern Pacific Ocean ($120^\circ\text{E} - 120^\circ\text{W}$) in April (left panel) and May (right panel) 2001. MODIS values are shown in + signs. The differences are shown to be larger in April as opposed to May because of more dust outbreaks in April versus May. CMAQ results are obtained via EPA ICAP-3 project (thanks to D. Roy and Carey Jang, EPA).

Results and Discussions

Case Selection and Experiment

We choose May 9, 2006 based upon a DC-8 flight, on which day airborne lidars confirmed elevated aerosols (dust and mixed aerosols), to conduct an experiment by changing the threshold of spatial variability used in MODIS cloud screening. In this experiment we set six thresholds, 0.0025 (operational), 0.002, 0.0015, 0.001, 0.0005, and 0.00025. Note that the last setting is an order of magnitude smaller compared to the operational one. Clearly, less and less AOD retrievals are seen with smaller thresholds (Figure 4). The MODIS operationally generated AOD product (upper left) depicts well-structured plumes (in the large circle) in yellow and orange color behind a frontal boundary. The dust-laden air is followed by air mass of mixed aerosols. The fine-mode fractions (FMF) obtained indicates that FMF values range from 0.1 to 0.35 for the dust dominated region (Figure 4 rightmost panel).

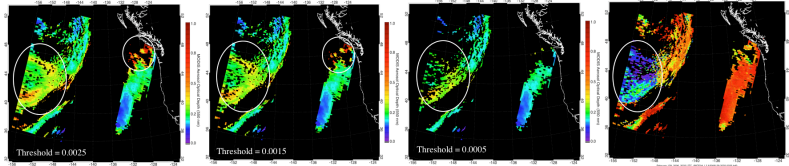


Figure 4. MODIS AOD retrievals on May 9, 2006 2025 UTC based upon three different thresholds for cloud screening using spatial variability (leftmost and central panels) and corresponding fine-mode fractions obtained (rightmost panel). Two circled areas are shown to represent dust over clouds (large circle) and cirrus clouds contamination (small circle).

The last DC-8 leg (upper left panel in Fig. 5) on May 9 before returning to base encountered dust plumes at the locations as circled (the large circle) in Fig. 4. The DC-8 onboard lidars detected elevated dust layers on that leg (right panel). The vertical distribution with dust above marine stratocumulus is also evident in the lidar image. The MODIS RGB image shows a wide area with marine stratocumulus behind a cold front underneath dust plumes. Reflectance of areas with the presence of dust above clouds tends to be darker, which can be seen in the RGB image. The RGB color needs to be adjusted more in order to visualize dust plumes more clearly. The distribution and the height of dust plumes were well predicted by a trajectory model (Brad Pierce, NASA LaRC) during flight planning of INTEX-B field campaign (not shown). The information of dust height obtained from both lidar observation and trajectory model forecast is consistent that the model serves as an alternative tool for studies in locations where lidar measurements were unavailable.

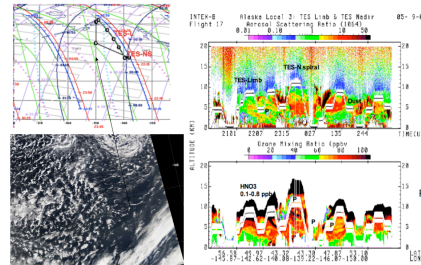


Figure 5. DC-8 flight route (upper left), MODIS RGB image (lower left) and DC-8 onboard lidar images of aerosol and ozone (right panel); courtesy of Ed. Browell.

Preliminary Radiative Forcing Calculations

MODIS-derived AODs, fine-mode fraction (FMF), and aerosol model selections are input into a fast radiative transfer model used by previous publication [Remer and Kaufman, 2006]. First, we compare aerosol radiative forcing (ARF) results with respect to different cloud-screening settings under cloud free conditions. Note that these comparisons of aerosol radiative forcing are focused on the changes in radiative forcing under cloud-free conditions, rather than the absolute values, with respects to different thresholds. The two regions selected for radiative forcing calculation show similar mean AOD (-0.3) but Region 1 appears to be dominated by dust aerosols (mean FMF -0.26) and Region 2 by mixed aerosols (mean FMF -0.55). (Region 2 is at the west of Region 1 that the geographical separation with dust ahead of urban/industrial pollution is reasonable). Table 1 displays the aerosol radiative forcing at top of the atmosphere (TOA). Region 2 is shown to have less cooling compared to Region 1, possibly due to the mixture with black carbon as mostly found in Asian pollution outflow and therefore absorbing more sunlight. The changes in the threshold show a maximum reduction in aerosol cooling by 2.2 watt/m^2 in Region 1 and 3.5 watt/m^2 in Region 2.

Table 1. Aerosol Radiative Forcing calculated at TOA in Region 1 and Region 2 under cloud-free condition.

Threshold	N	ARF-TOA	AOD-Mean	AOD-Std	FMF-Mean	FMF-Std
0.0025 - 1	2279	-19.6	0.31	0.08	0.26	0.20
0.0015 - 1	1986	-18.9	0.30	0.06	0.26	0.20
0.0005 - 1	1177	-18.3	0.27	0.05	0.29	0.19
0.00025 - 1	367	-17.4	0.25	0.05	0.37	0.16
0.0025 - 2	2184	-17.4	0.30	0.09	0.56	0.11
0.0015 - 2	1899	-16.7	0.29	0.09	0.57	0.11
0.0005 - 2	1149	-15.4	0.26	0.06	0.57	0.12
0.00025 - 2	277	-13.9	0.23	0.05	0.56	0.12

We also make an attempt to estimate radiative forcing with aerosol above clouds, for which we only use AODs derived by the original threshold (0.0025) but with assumptions of various cloud fractions (Table 2). The calculations are based upon cloud top and bottom at 800 and 900 mb, respectively, and an aerosol layer between 440 and 700 mb. The presence of clouds underneath an aerosol layer is significant in reducing aerosol cooling effect. Based upon the current threshold setting, the cloud-aerosol combined reduces cooling at least twice more effective than aerosol alone.

Table 2. Aerosol Radiative Forcing calculated at TOA with aerosols above clouds in Region 1.

Cloud Fraction	ARF-TOA (watt/m^2)	LWP (g/m^3)	Reff (μm)	ARF-TOA (watt/m^2)	LWP (g/m^3)	Reff (μm)
0.25	-14.6	42.5	8.2	-12.5	85.0	9.0
0.50	-9.75	42.5	8.2	-5.42	85.0	9.0
0.75	-4.83	42.5	8.2	-1.64	85.0	9.0
1.00	0.07	42.5	8.2	8.71	85.0	9.0

LWP: Cloud Liquid Water Path; Reff: Effect Radius of Cloud Droplet